AUTOMATIC EXTRACTION OF WRINKLE RIDGES IN VENUS MAGELLAN IMAGERY. M. T. Barata[1], E. I. Alves[1] and D. Vaz[1], Centre for Geophysics, Planetary Geosciences Group, University of Coimbra, Av. Dias da Silva, 3000-134 Coimbra, Portugal, mtbarata@gmail.com.

Introduction: Wrinkle ridges are interesting features and since they constitute the most abundant tectonic features on Venus, it is of great importance to understand some characteristics, such as orientation, length, among others. These parameters can be determinates in a simple way if the wrinkle ridges can be easily detected. The present work presents preliminary results of a method for the automatic detection of wrinkle ridges from Magellan SAR imagery at different scales.

Methodology: This work is based of the global distribution of the wrinkle ridges on Venus presented by [1]. As explained by the authors, the map was produced based on on-screen digital mapping of wrinkle ridges, from "browse" images of each C1-MIDRs (SAR images of Magellan, with 225 meters/pixel), to avoid the time-consuming process of digitalization. Also, they pointed the possibility to obtain other results in their work, if they had used images with better spatial resolution, such as the F-MIDRs (75 meters/pixel). Based on these aspects, this work presents the preliminary results of a method for automatic detection of wrinkle ridges based on fractal dimension and morphological transforms.

In Venus wrinkle ridges are long, narrow and sinuous features [2, 3], occurs in sets of evenly spaced, parallel ridges [2] and are radar bright when compared with the surfaces upon which they occur, as a consequence of their roughness. This can be observed in the image of figure 1. This image shows a Venusian plain with wrinkle ridges, located on Rusalka Planitia (the same image used in [2], with a geographic region common to the image used in [4, 5].

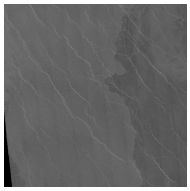

Figure 1 - Magellan image (C1-MIDR.00N180, framelet 19) of Rusalka Planita, Niobe Planitia. The image shows a characteristic plain, with a radar bright response of wrinkle ridge.

Due the ability of fractal analysis on the determination of the texture heterogeneity of the images, the methodology developed in this work starts with the calculation of fractal dimension, based on the method developed by Eastman [6]. The objective of this operation is to enhance the wrinkle ridges and simultaneously reduce the speckle on SAR images. Figure 2 shows the results of fractal dimension of the image of figure 1. By visual analysis of fractal image (figure 2(a)) wrinkle ridges shows higher fractal dimension ($D \geq 2.68$). Based on this value a threshold transform was performed, for values higher than D and the binary image obtained can be seen in figure 2(b). In this image wrinkle ridges are correctly identified, but the image is still noisy, due the speckle present on the original image. To distinguish the wrinkle ridges and correctly preserve their shape, the algorithm use mathematical morphology for binary images [**7**]. Thus, the fractal image was filtering by applying an area opening of size 16, followed by a reconstruction, to preserve the shape of the significant structures, as can be observed in fig 2(c).

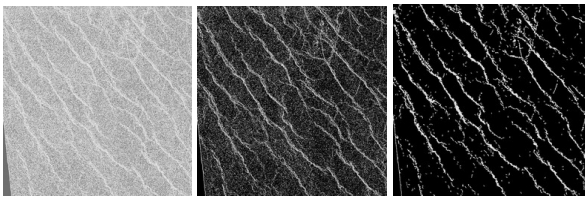

(a) (b) (c)

Figure 2 - (a) Fractal dimension of the image on fig. 1; (b) threshold of (a) based on fractal value for wrinkle ridges ($D \geq 2.68$); (c) area opening followed by reconstruction.

Now it is necessary to find the appropriate markers of wrinkle ridges. One way is through the distance function (figure 3(a)), since its allows to find the regional minima of the image to be used as markers of wrinkle ridges (figure 3(b)). The markers are very irregular and sometimes disconnected but these aspects can be minimize by applying a thickening, followed by dilation (figure 3 (c)).

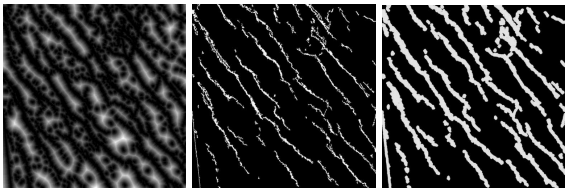

(a) (b) (c)

Figure 3 - (a) Distance function of figure 2 (c); (b) regional minima of distance function (markers of

wrinkle ridges); (c) thickness of the markers, followed by dilation.

The next step consists on performing an thinning, to reduce the thickness of the markers to one pixel. Figure 4(a) shows the final result of this operation and figure 4(b) the wrinkle ridges are superimposed on the original image.

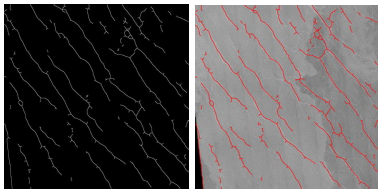

(a) (b)

Figure 4 - (a) Final result of automatic detection of wrinkle ridges; (b) superposition of the wrinkle ridges on the original image.

If the objective is to extracted the wrinkle ridges in different directions, the propose method continues by applying an ASF anisotropic filter, using a line with different directions as structuring element. An example of this approach can be observed in figures 5 (a), (b) for, respectively, the direction 135º and 45º, superimposed on the original image.

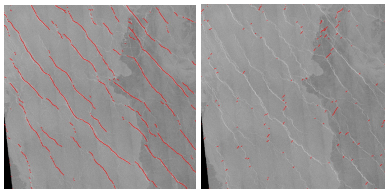

(a) (b)

Figure 5 - Wrinkle ridges in different directions: (a) direction 135º; (b) direction 45º.

This automatic method was also tested for FMDIR images. Since the speckle effect is stronger for this kind of images, before applying the algorithm, the original images are submitted to a low pass filter. The results of the application of the algorithm are shown in figure 6.

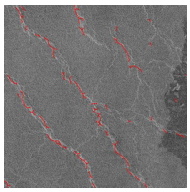

Figure 6 - Automatic extraction of wrinkle ridges superposition on the original image F-MIDR.05N177, framelet 52.

Conclusions: The aim of this work was the development of a methodology for automatically extracting wrinkle ridges of Venus imagery and the results obtained are very promising.

The great advantage of the propose method is the applicability to different scales without perform on-screen digitalization of wrinkle ridges. Therefore the results are less subjective and also less time-consuming. Another advantage is the extraction of other important characteristics of wrinkle ridges, such as geometric (length, size, orientation, and so on) parameters. Future work involve the integration of these parameters on the methodology, to perform a better characterization of all wrinkle ridges in Venus.

References: [1] Bilotti, F. and Suppe, J. (1999) *Icarus*, 139, 137-157. [2] Banerdt, W.B.. et al (1997) *Venus II – Geology, Geophysics, Atmosphere, and Solar Wind Environment*, 901-930. [3] Anderson, F. S. and Smrekar S. E., (1999) *JGR, 104(E12), 30743–30756*. [4] Solomon, S. C. et al. (1999) *Science*, 286, 87-90. [5] Solomon, S. C. et al. (1992) *JGR*, 97(E8), 13199–13255. [6] Eastman, J.R. (1985) in Annual Meeting of *Canadian Cartographic Association.* [7] Soille, P. (2002) *Morphological Image Analysis - Principles and Applications*. 2nd Ed..